World Journal of Advanced Research and Reviews
eISSN: 2581-9615 CODEN (USA): WJARAI
Cross Ref DOI: 10.30574/wjarr
Journal homepage: https://wjarr.com/

(RESEARCH ARTICLE)

Check for updates

Simulation of the Shallow Water Equations with Transmission Boundary Conditions in the Bay of Bengal Region

Md. Masum Murshed *

Department of Mathematics, University of Rajshahi, Rajshahi-6205, Bangladesh.

World Journal of Advanced Research and Reviews, 2025, 28(01), 1802-1815

Publication history: Received on 17 September 2025; revised on 22 October 2025; accepted on 25 October 2025

Article DOI: https://doi.org/10.30574/wjarr.2025.28.1.3633

Abstract

This study presents numerical simulations of the shallow water equations (SWEs) for the Bay of Bengal (BoB) using the Lagrange–Galerkin method (LGM) on a triangular mesh, with the transmission boundary conditions (TBCs). To examine the positional sensitivity of the transmission boundaries, the simulations are conducted with TBCs imposed at two distinct locations within the Bay of Bengal domain. The computed total mass and L^2-norm of the surface elevation η demonstrate that the transmission boundary condition performs efficiently and exhibits minimal dependence on its placement. These results indicate that the TBC is well-suited for modeling open-sea boundaries, ensuring smooth wave propagation without artificial reflection. The study serves as a foundational step toward developing an accurate and stable storm surge prediction framework for the Bay of Bengal using the Lagrange–Galerkin approach.

Keywords: Shallow Water Equations; Transmission Boundary Conditions; Bay of Bengal; Lagrange–Galerkin Method; Numerical Simulation

1. Introduction

The Shallow Water Equations (SWEs) form a coupled system consisting of a pure convection equation for the total wave height, denoted by ϕ, and a simplified Navier–Stokes equation for the horizontal velocity $u = (u_1, u_2)^T$, obtained by depth-averaging the flow in the vertical (x_3) direction. These equations are widely used to model large-scale geophysical flows, such as tsunamis and storm surges, particularly in coastal and bay regions where accurate wave propagation is crucial.

In numerical simulations of such phenomena, suitable boundary conditions at the open-sea boundaries are essential to prevent non-physical reflections when waves reach these boundaries (see **Figure 1**). To achieve this, *Transmission Boundary Conditions (TBCs)*, as introduced in [4], are imposed on the open-sea boundaries Γ_T. These conditions allow outgoing waves to exit the computational domain smoothly by minimizing artificial reflections. The TBC is expressed as:

$$u(x,t) = c(x)\frac{\eta(x,t)}{\phi(x,t)}n(x), \qquad \ldots. \qquad (1)$$

where $c(x)$ is a positive coefficient, $\eta(x,t) = \phi(x,t) - \zeta(x)$ represents the free surface elevation from a reference level determined by the depth function $\zeta(x)$, and $n(x)$ denotes the unit outward normal vector to the boundary.

A number of studies [1–3, 9–15] have investigated storm surge and tidal simulations in the Bay of Bengal (BoB), which borders the coasts of Bangladesh and eastern India. Most of these models employ radiation-type boundary conditions to treat open-sea boundaries, which are mathematically similar to TBCs as described in [4]. However, as noted in [7],

* Corresponding author: Md. Masum Murshed

TBCs generally produce more stable and physically accurate results for SWEs compared to traditional radiation conditions. In [5], both theoretical and numerical stability analyses for SWEs with TBCs were performed using finite difference methods (FDM). While FDM is suitable for regular domains, such as rectangular grids, it becomes inefficient for realistic oceanic geometries that feature complex coastlines. In these cases, the finite element method (FEM), particularly with triangular meshing, offers greater flexibility and precision (see **Figure 1**).

Figure 1 The Bay of Bengal and the coastal region of Bangladesh

The *Lagrange–Galerkin Method (LGM)* combines the strengths of FEM with a time-discretization technique based on the material derivative,

$$\frac{\phi^{k+1}(x) - \phi^{k}(x - u^{k}(x)\Delta t)}{\Delta t},$$

Where the upwind point $x - u^{k}(x)\Delta t$ is used for numerical evaluation. If this point lies outside the computational domain, the nearest boundary value of ϕ^{k} is adopted. Unlike FDM, which can fail when $u^{k+1} \cdot n < 0$ due to missing boundary data, LGM remains stable and effective under such conditions.

In this study, numerical experiments are conducted to test how the performance of the transmission boundary condition depends on its spatial placement. The TBC is applied at two distinct positions within the Bay of Bengal to examine its robustness. The results confirm that the transmission boundary condition works efficiently and shows minimal sensitivity to its position.

To the best of our knowledge, no previous work has implemented the Lagrange–Galerkin method for storm surge simulation in the Bay of Bengal. Therefore, this research provides a significant step toward developing a reliable and accurate storm surge prediction model for this region using LGM with transmission boundary conditions.

The paper is organized as follows: Section 2 introduces the mathematical formulation of the problem. Section 3 describes the Lagrange–Galerkin numerical scheme. Section 4 presents the simulation results. Finally, Section 5 discusses the findings and concludes the study.

2. Statement of the problem

Following the formulation presented in [5], the mathematical model considered in this study is based on the two-dimensional Shallow Water Equations (SWEs). Let $\Omega \subset \mathbb{R}^2$ be a bounded domain, and let $T > 0$ be a fixed time. The objective is to find $(\phi, u) : \overline{\Omega} \times [0, T] \to \mathbb{R} \times \mathbb{R}^2$ such that

$$\begin{cases} \dfrac{\partial \phi}{\partial t} + \nabla \cdot (\phi u) = 0 & \text{in } \Omega \times (0,T), \\ \rho\phi\left[\dfrac{\partial u}{\partial t} + (u \cdot \nabla)u\right] - 2\mu\nabla \cdot \big(\phi D(u)\big) + \rho g \phi \nabla \eta = 0 & \text{in } \Omega \times (0,T), \\ \phi = \eta + \zeta & \text{in } \Omega \times (0,T), \end{cases} \tag{2}$$

subject to the boundary conditions

$$u = 0 \qquad \text{on} \quad \Gamma_D \times (0,T), \tag{3}$$

$$u = c\frac{\eta}{\phi}n \qquad \text{on} \quad \Gamma_T \times (0,T), \tag{4}$$

and initial conditions

$$u = u^0, \quad \eta = \eta^0 \qquad \text{in } \Omega, \text{ at } t = 0, \tag{5}$$

where ϕ denotes the total water height, and $u = (u_1, u_2)^T$ represents the horizontal velocity vector. The variable $\eta: \overline{\Omega} \times [0,T] \to \mathbb{R}$ corresponds to the free surface elevation relative to the reference level, while $\zeta(x) > 0 \ (x \in \overline{\Omega})$ denotes the undisturbed water depth measured from that reference level (see **Figure 2**).

The strain-rate tensor is defined as

$$D(u) := \frac{\nabla u + (\nabla u)^T}{2},$$

and n is the outward unit normal vector on the boundary $\partial\Omega$. The boundary $\Gamma := \partial\Omega$ consists of two disjoint parts: the Dirichlet boundary Γ_D and the transmission boundary Γ_T such that

$$\overline{\Gamma} = \overline{\Gamma}_D \cup \overline{\Gamma}_T, \ \Gamma_D \cap \Gamma_T = \emptyset.$$

The Dirichlet boundary condition is imposed along the coastline, while the transmission boundary condition (TBC) is applied to the open-sea boundary to allow outgoing waves to exit the domain smoothly without artificial reflections.

The physical constants are defined as follows: $\rho > 0$ is the density of water, $\mu > 0$ is the dynamic viscosity, and $g > 0$ is the acceleration due to gravity. The coefficient $c(x)$ appearing in the transmission condition is given by

$$c(x) := c_0\sqrt{g\zeta(x)},$$

where c_0 is a positive constant.

Throughout this study, it is assumed that $\zeta \in C^1(\overline{\Omega})$.

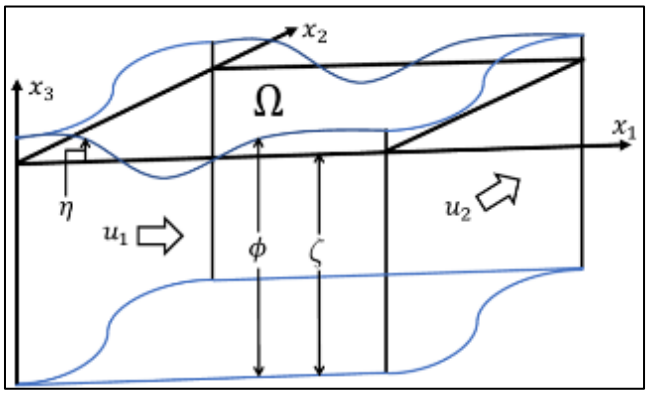

Figure 2 Model domain (see [5])

3. LG scheme

Following the formulation presented in [5], a Lagrange–Galerkin (LG) numerical scheme is considered to approximate the shallow water equations.

Let $\mathcal{T}_h = \{K\}$ denote a triangulation of the domain Ω, and M_h be the standard P1 (piecewise linear) finite element space. We define

$$\Psi_h := M_h$$

or the water surface elevation η, and

$$V_h(\psi_h) := \left\{ v_h \in M_h^2 \middle| \begin{matrix} v_h(Q) = 0, & \forall Q \text{ being a node on } \Gamma_D \\ v_h(P) = c(P)\frac{\psi_h(P)-\zeta(P)}{\psi_h(P)} n(P), & \forall P \text{ being a node on } \Gamma_T \end{matrix} \right\},$$

or the velocity field u. The goal of the LG scheme is to determine a sequence

$$\left\{\left(\phi_h^k, u_h^k\right)\right\}_{k=1}^{N_T} \subset \Psi_h \times V_h$$

such that, for each time step $k = 1, \dots, N_T$, the following system holds:

$$\begin{cases} \displaystyle\int_\Omega \frac{\phi_h^k - \widetilde{\phi_h^{k-1}} \circ X_{1h}^{k-1} \gamma_h^{k-1}}{\Delta t} \psi_h dx = 0, & \forall \psi_h \in \Psi_h, \\ \displaystyle\rho \int_\Omega \phi_h^k \frac{u_h^k - \widetilde{u_h^{k-1}} \circ X_{1h}^{k-1}}{\Delta t} \cdot v_h dx + 2\mu \int_\Omega \phi_h^k D\left(u_h^k\right) : D(v_h) dx \ + \rho g \int_\Omega \phi_h^k \nabla \eta_h^k \cdot v_h dx = 0, & \forall v_h \in V_h, \\ \phi_h^k = \eta_h^k + \Pi_h^{FEM} \zeta. \end{cases} \tag{6}$$

Here, the mapping $X_{1h}^k : \Omega \to \Omega$ is defined as

$$X_{1h}^k(x) := x - u_h^k(x)\Delta t,$$

and $\gamma_h^k(x) := \det\left(\frac{\partial X_{1h}^k(x)}{\partial x}\right)$ denotes the Jacobian determinant of the transformation. The composition symbol "$\circ$" represents the functional composition, i.e.

$$\left[v_h \circ X_{1h}^k\right](x) := v_h\left(X_{1h}^k(x)\right).$$

The operator $\Pi_h^{\mathrm{FEM}} : C\left(\overline{\Omega}\right) \to M_h$ is the standard Lagrange interpolation operator. The extension of a finite element function ψ_h to the entire plane $\mathbb{R}^2$ is defined as

$$\widetilde{\psi_h}(x) = \begin{cases} \psi_h(x), & x \in \overline{\Omega}, \\ \psi_h(P_x), & x \in \mathbb{R}^2 \setminus \overline{\Omega}, \end{cases}$$

where $P_x \in \Gamma$ is the nearest nodal point to x.

At each time step, the first equation in system (6) is used to determine $\phi_h^k \in \Psi_h$. Then, using this computed ϕ_h^k, the second equation is solved to obtain the velocity $u_h^k \in V_h$.

The first equation of (6) employs the concept of a mass-conservative Lagrange–Galerkin scheme as proposed in [16], ensuring numerical stability and conservation of mass throughout the simulation.

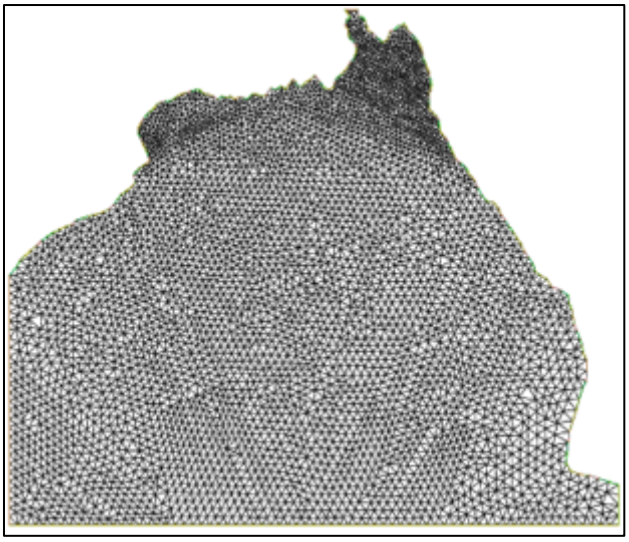

Figure 3 A triangular mesh for the Bay of Bengal

4. Numerical results

This section presents the numerical experiments conducted to validate the proposed Lagrange–Galerkin (LG) scheme for the shallow water equations

4.1. Simulation Results for the Bay of Bengal

In this subsection, the simulation results for the Bay of Bengal region are discussed using the LG scheme introduced in Section 3. For computational simplicity, the actual geographical domain was slightly modified, and a triangular mesh was constructed as illustrated in **Figure 3**, following the approach in [6]. The complete setup of the numerical simulation is shown in **Figure 4**, and the computational domain is denoted by Ω.

The horizontal extent of the domain ranges from 0 km to 1051.4 km, while the vertical extent covers 0 km to 889.59 km. Two types of boundary conditions were applied:

- **Zero Dirichlet boundary condition** on Γ_D, representing the coastal boundary; and
- **Transmission boundary condition** on Γ_T, representing the open-sea region.

As illustrated in **Figure 4**, the transmission boundary Γ_T is composed of three distinct segments:

$$AB = \Gamma_{T_1}, \qquad BC = \Gamma_{T_2}, \qquad CD = \Gamma_{T_3}.$$

The initial water surface elevation is prescribed as

$$\eta^0 = 0.05e^{-0.1|x-p|^2},$$

where p denotes the nodal point nearest to the coordinates (525, 440).

The simulation was performed using the following parameter values:

$$\zeta = 2.0,\ \mu = 1,\ g = 9.8 \times 10^{-3},\ \rho = 10^{12},\ c_0 = 0.9,\ h = 1.408044,\ T = 5000\text{s}.$$

The results obtained at different time levels $t = 0$s, 2800s, 3120s, 3240s, 3740s, 3940s, and 4660s are shown in the left panels of **Figures 6** and **7**. From these figures, it is observed that a circular wave is generated near the **center** of the domain and propagates outward over time. When the wavefront reaches the coastal boundary Γ_D, partial reflection occurs, while at the transmission boundary Γ_T, almost no reflection is detected. This demonstrates that the wave energy is smoothly transmitted through Γ_T, confirming the effectiveness of the transmission boundary condition for open-sea flow simulation.

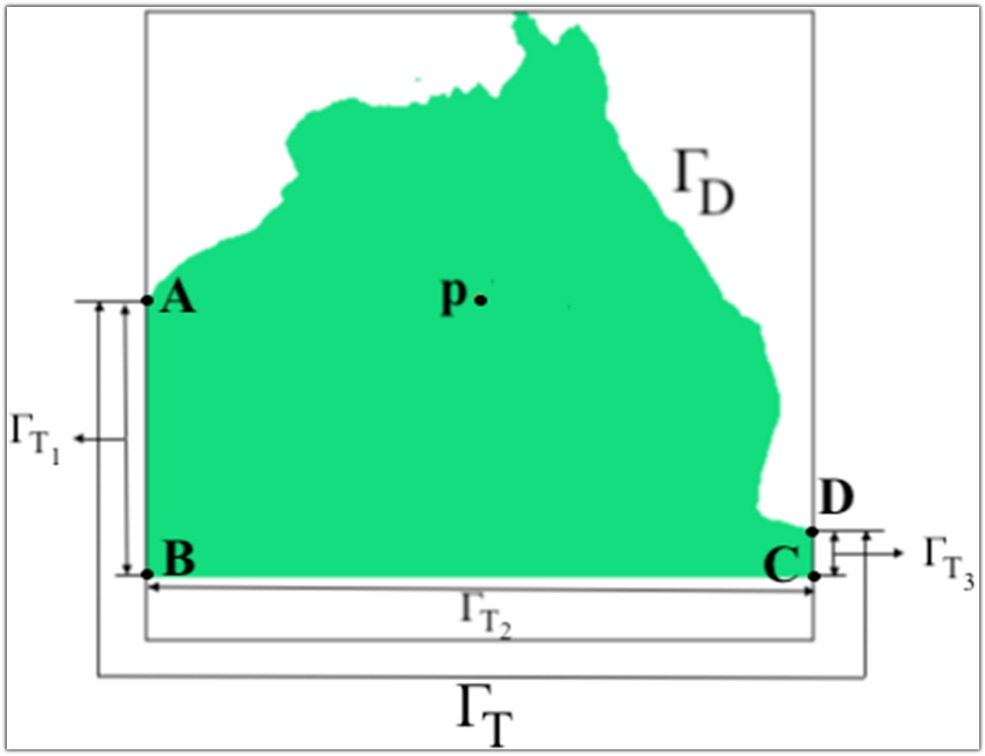

Figure 4 A figure of Bay of Bengal domain showing the setting of the transmission and the Dirichlet boundaries

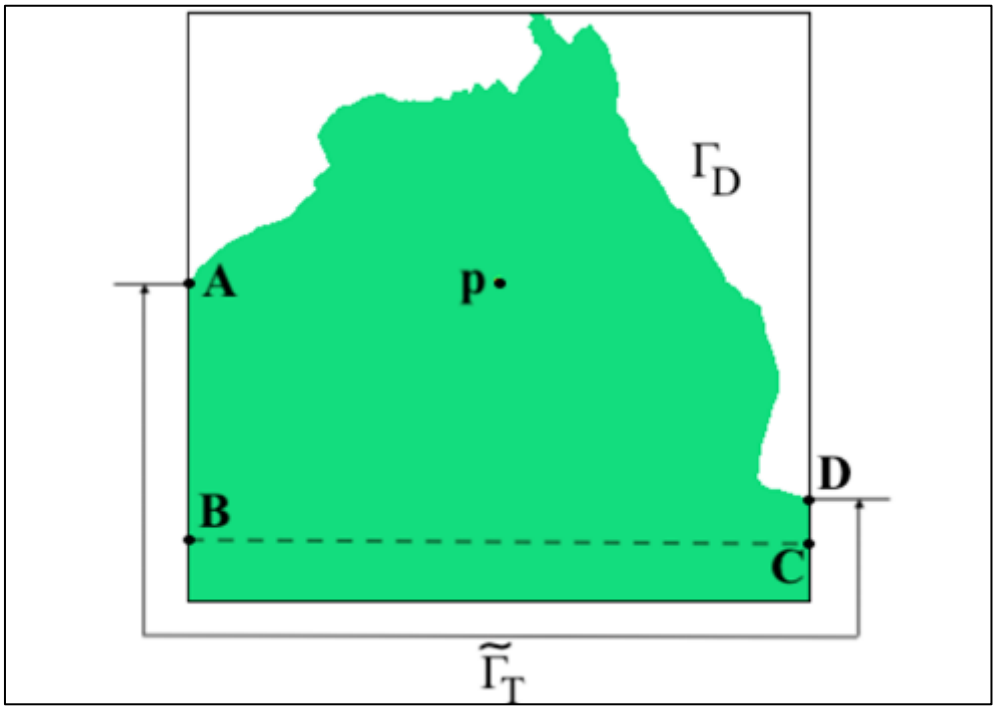

Figure 5 A figure of extended domain showing the setting of the transmission and the Dirichlet boundaries

We also investigated the effect of slightly modifying the position of the transmission boundary. To do so, an extended domain $\widetilde{\Omega}$ was constructed by enlarging Ω by 100 km in the negative vertical direction, as shown in **Figure 5**. Consequently, $\widetilde{\Omega}$ extends from 0 km to 1051.4 km horizontally and from −100 km to 889.59 km vertically, with $\Omega \subset \widetilde{\Omega}$. The Dirichlet boundary Γ_D remains the same for both domains, while Γ_T denotes the transmission boundary of Ω.

A numerical simulation was then performed in the extended domain $\widetilde{\Omega}$ using the same parameter settings as before. The results at $t = 0$s, 2800s, 3120s, 3240s, 3740s, 3940s, and 4660s are presented in the right panels of **Figures 6** and **7**.

The behavior of the wave propagation in $\widetilde{\Omega}$ closely resembles that observed in Ω, confirming that the transmission boundary condition remains stable and effective even when its position is slightly modified. From both sets of results (left and right panels of **Figures 6** and **7**), it is evident that the proposed LG scheme accurately reproduces the physical behavior of wave transmission in the open-sea region of the Bay of Bengal.

4.2. Computation of Mass and L^2 Norm for the Bay of Bengal

This section presents the computation of the total mass and the L^2 norm of the surface elevation for the Bay of Bengal

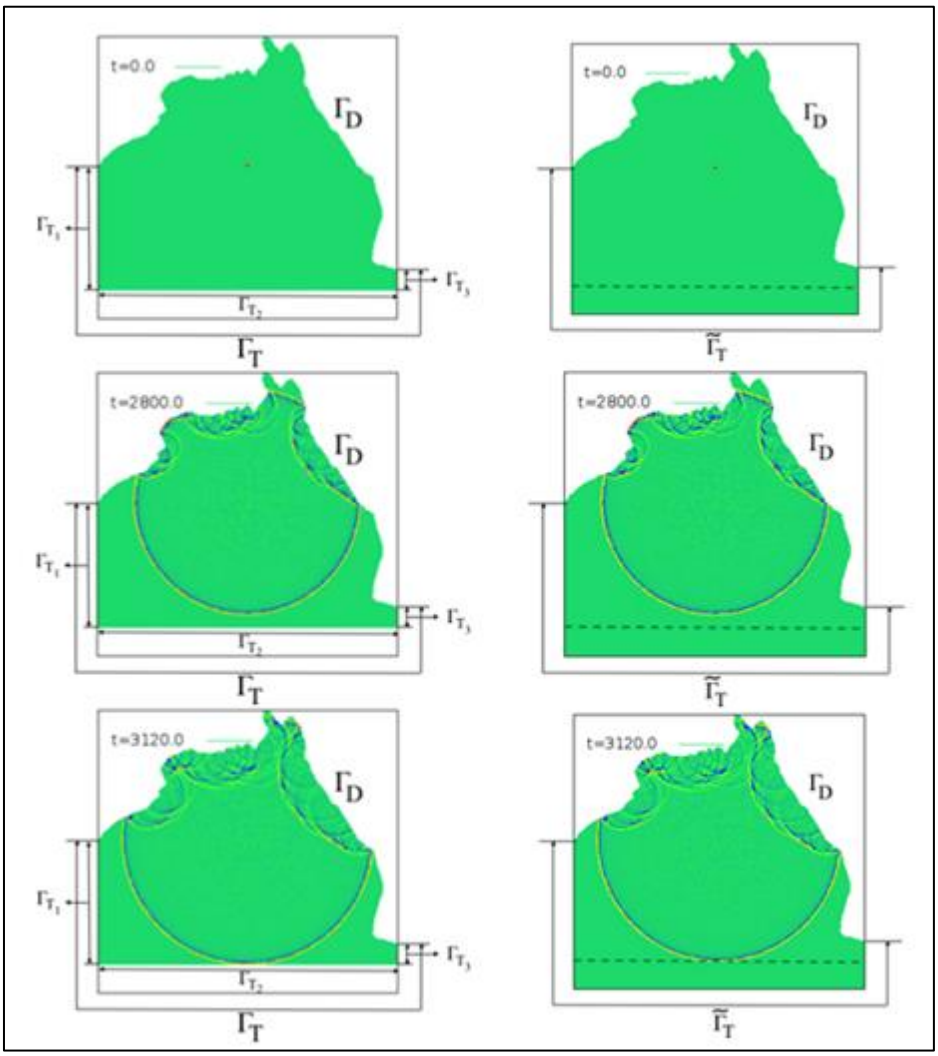

Figure 6 Simulation of SWEs in the Bay of Bengal at time $\boldsymbol{t = 0s, 2800s}$, and $\boldsymbol{3120s}$

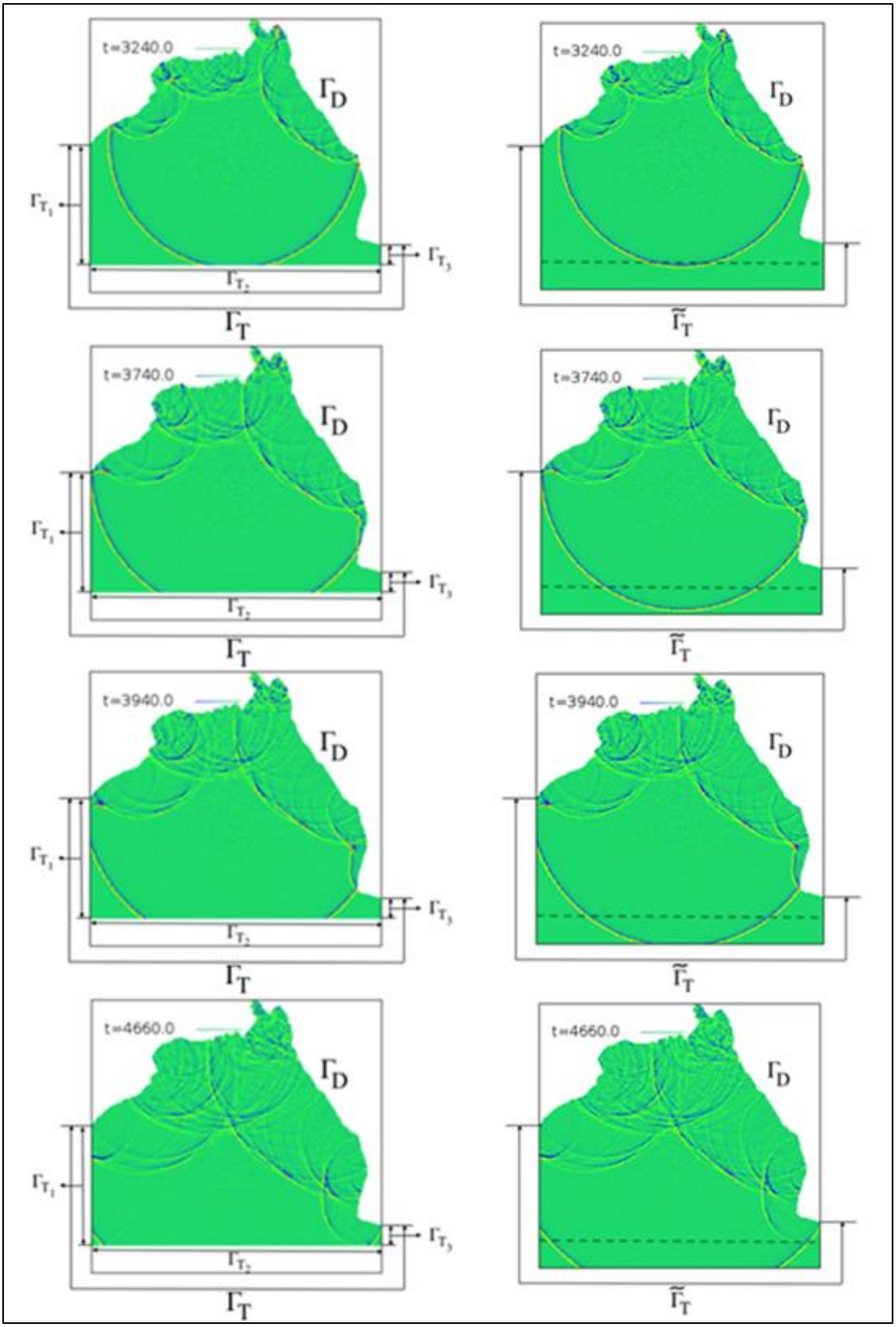

Figure 7 Simulation of SWEs in the Bay of Bengal at time $\boldsymbol{t = 3240s, 3740s, 3940s}$ and $\boldsymbol{4660s}$

4.2.1. Computation of Mass

The total mass M(t) at time tis defined as

$$\boldsymbol{M(t) := \int_{\Omega} \eta(x,t)\, dx \approx \int_{\Omega} (\Pi \eta_h^k)\, dx =: M_h^k,}$$

where $\boldsymbol{t = t^k}$ $(\boldsymbol{k \geq 0,\ k \in \mathbb{Z}})$, and the integration is performed over the common part of the domains $\boldsymbol{\Omega}$ and $\boldsymbol{\widetilde{\Omega}}$. It should be noted that in the domain $\boldsymbol{\Omega}$, the boundaries AB, BC, and CD serve as transmission boundaries, whereas in the extended domain $\boldsymbol{\widetilde{\Omega}}$, the segment BC lies within the domain (see **Figures 4** and **5**). The computed mass variation with time is displayed in **Figure 8**.

The time derivative of the mass is given by

$$\begin{aligned} M'(t) &= \int_{\Omega} \frac{\partial \eta}{\partial t}(x,t)\, dx \\ &= \int_{\Omega} \frac{\partial \phi}{\partial t}(x,t)\, dx \text{ (from the third equation of (2) and } \zeta = \text{constant)} \\ &= -\int_{\Omega} \nabla \cdot (\phi u) dx \text{ (from the first equation of (2))} \\ &= -\int_{\partial\Omega} (u \cdot n)\phi ds = -\int_{\Gamma_D \cup \Gamma_T} (u \cdot n)\phi ds = -\int_{\Gamma_T} (u \cdot n)\phi ds \\ &= -\int_{\Gamma_T} c\eta ds \text{ (from the equation (4), here } c \text{ is a constant)} \end{aligned}$$

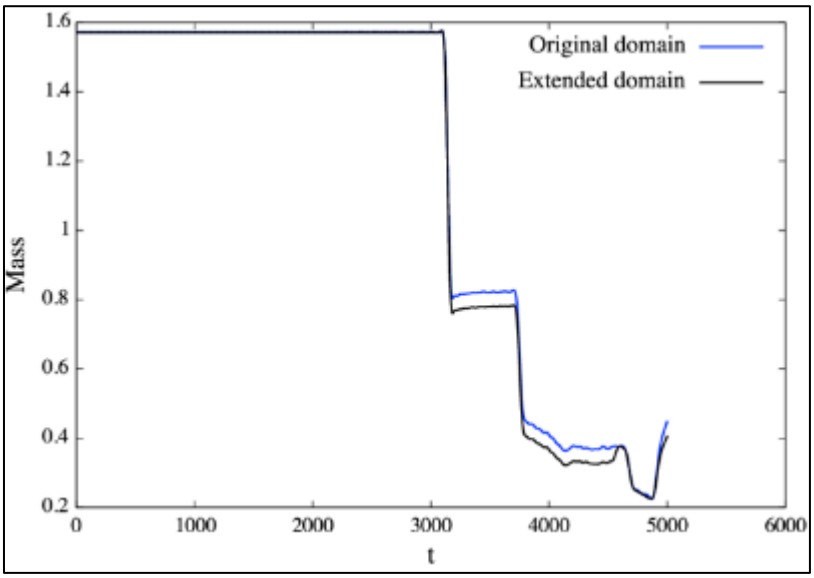

Figure 8 Graphs of $\boldsymbol{M_h^k}$ versus $\boldsymbol{t = t^k}$ $(\boldsymbol{\geq 0,\ k \in \mathbb{Z}})$ for the common part of the domains $\boldsymbol{\Omega}$ and $\boldsymbol{\widetilde{\Omega}}$

From this relation, it follows that the variation of the total mass depends on the sign of η along the transmission boundary Γ_T:

- If $\eta > 0$ on Γ_T, the total mass decreases;
- If $\eta < 0$ on Γ_T, the total mass increases.

To better understand this behavior, the distributions of η along the boundary segments AB, BC, and CD are plotted for both domains Ω and $\widetilde{\Omega}$ in **Figures 9** and **10**, complementing the mass evolution shown in **Figure 8**.

The results presented in **Figures 6–10** correspond to times$t = 0$s, 2800s, 3120s, 3240s, 3740s, 3940s and 4660s. The following observations can be made:

- Up to approximately $t = 3100s$, the total mass remains nearly constant, indicating that the wave has not yet interacted with the transmission boundary.
- Around $t = 3120s$, a significant drop in mass is observed as the wave reaches the boundary Γ_{T_2} (see **Figure 6**). At this moment, η is positive on Γ_T (**Figure 9**).
- Between $3200s$ and $3700s$, the mass remains nearly stable due to the partial cancellation of positive and negative η values along Γ_T (**Figure 10**, $t = 3240s$).

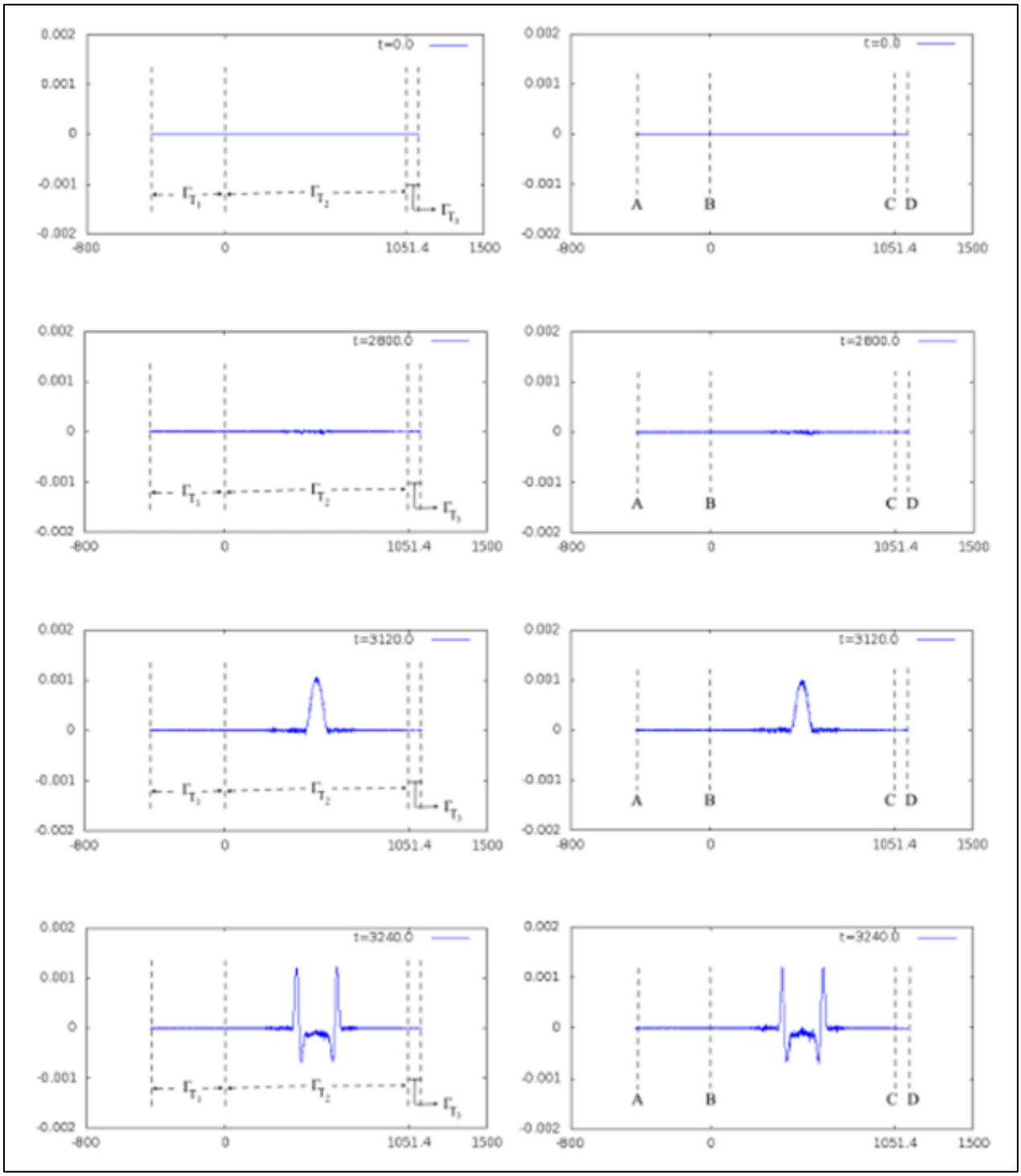

Figure 9 Graph of $\boldsymbol{\eta}$ on AB, BC and CD for both $\boldsymbol{\Omega}$ and $\widetilde{\boldsymbol{\Omega}}$ at time $\boldsymbol{t = 0s, 2800s, 3120s}$, and $\boldsymbol{3240s}$

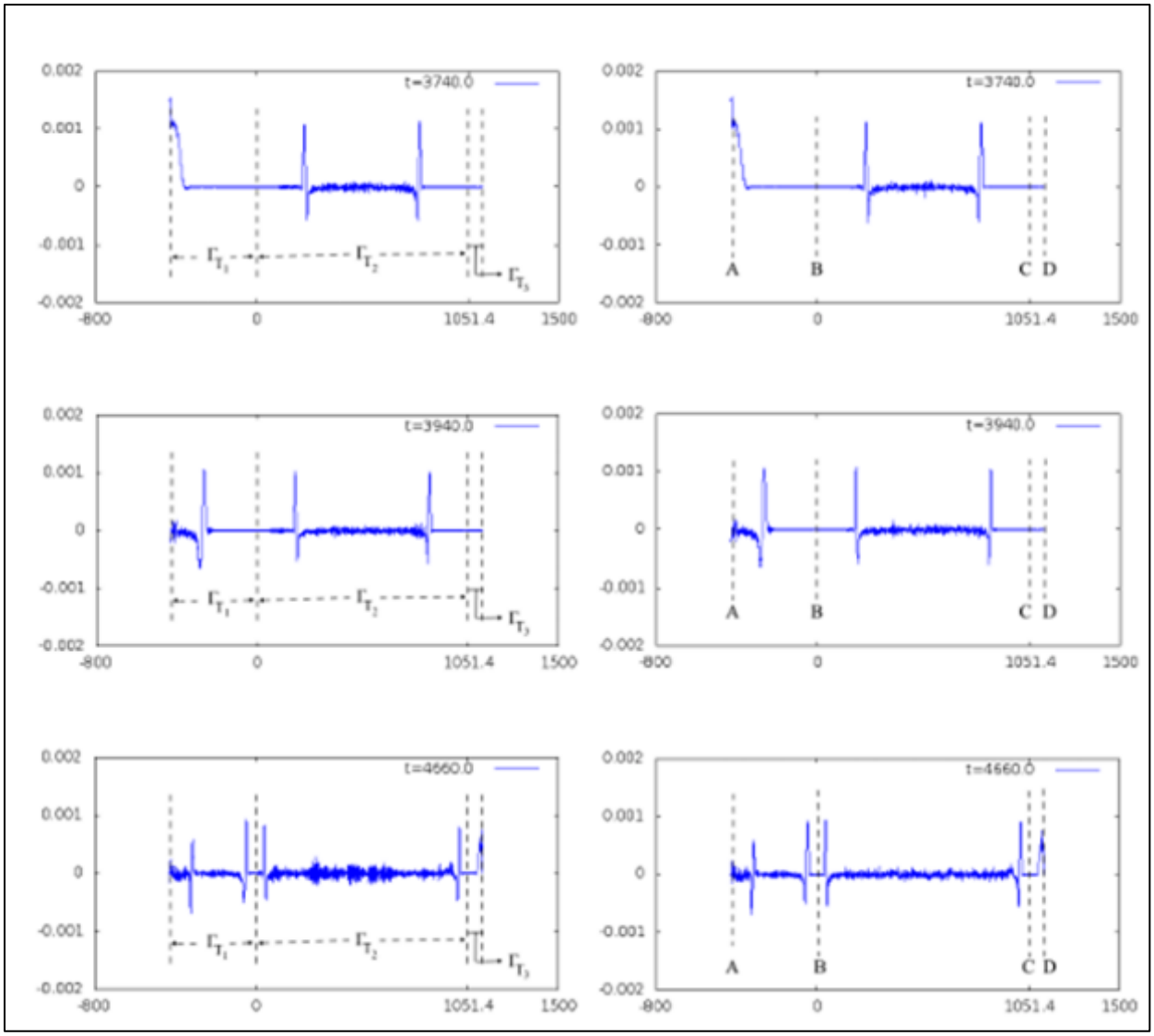

Figure 10 Graph of $\boldsymbol{\eta}$ on AB, BC and CD for both $\boldsymbol{\Omega}$ and $\widetilde{\boldsymbol{\Omega}}$ at time $\boldsymbol{t = 3740s}$, $\boldsymbol{3940s}$ and $\boldsymbol{4660s}$

- A second major decay occurs near $t = 3740s$, corresponding to the wave's interaction with Γ_{T_1} (**Figure 7**). Again, η is positive on Γ_T at this instant (**Figure 10**).
- Between $3800s$ and $4650s$, a gradual mass decrease is observed as η remains positive along Γ_T (**Figure 10**, $t = 3940s$).
- Finally, a third sharp decline in mass occurs around $t = 4660s$, when the wave reaches the boundary Γ_{T_3} (**Figure 7**), where η is again positive (**Figure 10**).
- It should be noted that a small degree of artificial reflection still occurs at the transmission boundary, which accounts for the minor differences between the mass curves obtained for the two domains ($\boldsymbol{\Omega}$ and $\widetilde{\Omega}$) in **Figure 8**.

4.2.2. Computation of the L^2 Norm

The L^2 norm of the surface elevation η, has been computed to assess the overall energy distribution of the wave within the domain. It is defined as

$$\| \eta(t) \|_{L^2} := \sqrt{\int_\Omega | \eta(x,t) |^2 \, dx} \approx \sqrt{\int_\Omega | \Pi\eta_h^k |^2 \, dx} =: \| \eta_h^k \|_{L^2},$$

where $t = t^k$ ($\geq 0,\ k \in \mathbb{Z}$) and the integration is performed over the common region of the domains $\boldsymbol{\Omega}$ and $\widetilde{\Omega}$. **Figure 11**, presents the computed L^2 norms for both domains. The results indicate that the two curves are almost identical, confirming that the transmission boundary condition does not introduce any significant numerical instability or artificial reflection in the wave energy.

From the series of simulations illustrated in Figures **6-11**, it can be observed that the transmission boundary condition effectively allows outgoing waves to pass through the open-sea boundary with minimal reflection. Additionally, when the location of the transmission boundary is slightly modified—by extending the domain downward by 100 km (as described earlier)—the computed L^2 norms and mass values remain consistent in the common region of the domains $\boldsymbol{\Omega}$ and $\widetilde{\Omega}$.

These results demonstrates that the proposed Lagrange–Galerkin (LG) numerical scheme provides a reliable and accurate simulation of wave propagation in the Bay of Bengal. The variation between results obtained from the original and extended domains is within an acceptable error margin of approximately 5%, which confirms the robustness and precision of the method used in this study.

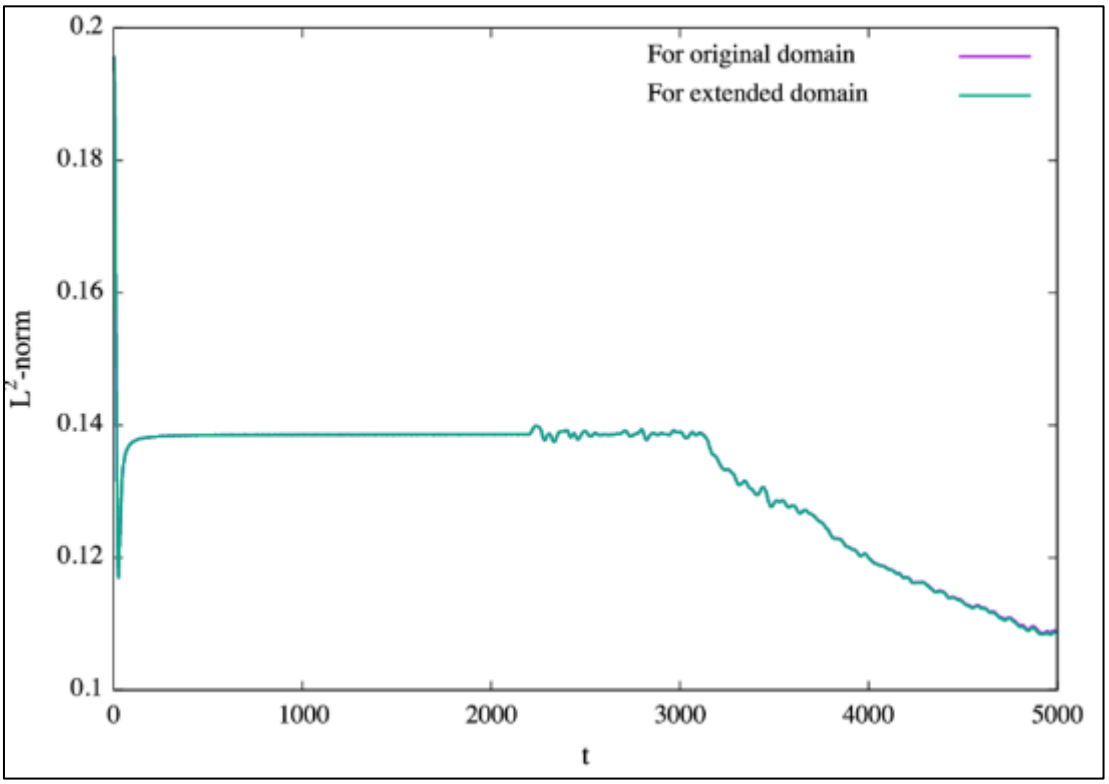

Figure 11 $\| \eta_h^k \|_{L^2}$ versus $t = t^k$ ($\geq 0,\ k \in \mathbb{Z}$) for the common part of the domains $\boldsymbol{\Omega}$ and $\widetilde{\Omega}$

5. Result and discussion

In this study, we have presented the results of numerical simulations of the Shallow Water Equations (SWEs) over the Bay of Bengal (BoB) domain using the Lagrange–Galerkin (LG) scheme described in **Section 3**. The simulations were performed for two different boundary configurations, as illustrated in **Figures 6** and **7**.

The results show that a circular wave is generated near the center of the domain, which propagates outward as time progresses. When the wavefront encounters the Dirichlet boundary Γ_D, partial reflection occurs. However, when it reaches the transmission boundary Γ_T, almost no reflection is observed. This indicates that the transmission boundary allows the wave to exit the computational domain smoothly, validating the effectiveness of the transmission boundary condition.

We further computed the total mass of η for both boundary configurations. The results, shown in **Figure 8**, reveal a gradual decay in mass over time, primarily due to the wave's interaction with the transmission boundary. This demonstrates that the transmission boundary condition works well from a numerical standpoint.

Similarly, the L^2 norms of η, corresponding to the two boundary configurations described in **Subsection 4.1**, are presented in **Figure 11**. The curves are almost identical, confirming that the transmission boundary condition remains stable and largely unaffected by small changes in its position.

From **Figures 6-11**, it can be concluded that the transmission boundary condition performs effectively in all cases considered. Even when the transmission boundary is slightly displaced, the overall wave behavior, including mass and energy evolution, remains nearly unchanged. This stability highlights the robustness of the LG scheme in simulating open-sea wave propagation in the Bay of Bengal region.

6. Conclusion

The numerical simulations presented in this study demonstrate that the transmission boundary condition (TBC), when applied to the Shallow Water Equations (SWEs) using the Lagrange–Galerkin (LG) method on a triangular mesh, effectively allows wave propagation in the Bay of Bengal without generating artificial reflections. The results confirm that the TBC performs efficiently and remains nearly independent of its spatial placement, ensuring numerical stability and physical consistency in open-sea modelling. The slight decay in total mass and stable $\boldsymbol{L^2}$-norm of surface elevation further validate its robustness. Overall, this research establishes the Lagrange–Galerkin approach as a reliable framework for simulating shallow water dynamics with realistic boundary treatments. The outcomes of this study will contribute to the development of more accurate and efficient storm surge prediction models for the Bay of Bengal, ultimately aiding in coastal disaster preparedness and protection of vulnerable communities.

Compliance with ethical standards

The author declares that this study was conducted in accordance with ethical research practices. No human participants or animals were involved in the study, and hence no ethical approval was required. The author further confirms that there are no conflicts of interest, financial or otherwise, that could have influenced the results or interpretations presented in this work. All sources of data and references have been properly acknowledged.

Acknowledgments

The author gratefully acknowledges the referees for their valuable comments and constructive suggestions, which have significantly improved this manuscript. Special thanks are also extended to Mr. Kouta Futai, Professor Masato Kimura, and Professor Hirofumi Notsu for their continuous guidance and assistance in preparing the results. This research was financially supported by the Dean of the Faculty of Science, University of Rajshahi, under Grant No. A-721/5/52/RU/Science-04/2024-2025.

Disclosure of conflict of interest

The author declares that there are no conflicts of interest associated with this publication.

References

[1] P. K. Das, Prediction model for storm surges in the Bay of Bengal, Nature, 239 (1972), 211—213.

[2] S. K. Debsarma, Simulations of storm surges in the Bay of Bengal, Marine Geodesy, 32 (2009), 178—198.

[3] B. Jonhs and A. Ali, The numerical modeling of storm surges in the Bay of Bengal, Quarterly Journal of the Royal Meteorological Society, 106 (1980), 1—18.

[4] H. Kanayama and H. Dan, Tsunami propagation from the open sea to the coast, Tsunami, Chapter 4, Intech Open, (2016), 61—72.

[5] M. M. Murshed, K. Futai, M. Kimura and H. Notsu (2021), Theoretical and numerical studies for energy estimates of the shallow water equations with a transmission boundary condition, Discrete Contin. Dyn. Syst. Ser. S. 14(3): 1063–1078.

[6] M. M. Murshed, M. M. B. Shiraj, S. Ullah, M. M. Rahman, M. Hossain (2023), On the Approximation of the Bay of Bengal Domain to be Compatible for the Implementation of Finite Element Method, Wor. J. Adv. Eng. Tec. Sci. 09(01), 290–295.

[7] M. M. Rasid, M. Kimura, M. M. Murshed, E. R. Wijayanti and H. Notsu (2023), A Two-Step Lagrange–Galerkin Scheme for the Shallow Water Equations with a Transmission Boundary Condition and Its Application to the Bay of Bengal Region Part I: Flat Bottom Topography, Mathematics 11(7), 1633.

[8] G. C. Paul and A. I. M. Ismail, Tide surge interaction model including air bubble effects for the coast of Bangladesh, Journal of the Franklin Institute, 349 (2012), 2530—2546.

[9] G. C. Paul and A. I. M. Ismail, Contribution of o shore islands in the prediction of water levels due to tide-surge interaction for the coastal region of Bangladesh, Natural Hazards, 65 (2013), 13—25.

[10] G. C. Paul, A. I. M. Ismail and M. F. Karim, Implementation of method of lines to predict water levels due to a storm along the coastal region of Bangladesh, Journal of Oceanography, 70 (2014), 199—210.

[11] G. C. Paul, M. M. Murshed, M. R. Haque, M. M. Rahman and A. Hoque, Development of a cylindrical polar coordinates shallow water storm surge model for the coast of Bangladesh, Journal of Coastal Conservation, 21 (2017), 951—966.

[12] G. C. Paul, S. Senthilkumar and R. Pria, Storm surge simulation along the Meghna estuarine area: An alternative approach, Acta Oceanologica Sinica, 37 (2018), 40—49.

[13] G. C. Paul, S Senthilkumar and R. Pria, An efficient approach to forecast water levels owing to the interaction of tide and surge associated with a storm along the coast of Bangladesh, Ocean Engineering, 148 (2018), 516—529.

[14] G. D. Roy, A. B. M. Humayun Kabir, M. M. Mandal and M. Z. Haque, Polar coordinate shallow water storm surge model for the coast of Bangladesh, Dynamics of Atmospheres and Oceans, 29 (1999), 397—413.

[15] G. D. Roy and A. B. H. M. Kabir, Use of nested numerical scheme in a shallow water model for the coast of Bangladesh, BRAC University Journal, 1 (2004), 79—92.

[16] H. X. Rui and M. Tabata, A mass-conservative characteristic finite element scheme for convection-diffusion problems, Journal of Scientific Computing, 43 (2010), 416—432.